(CONF-881014--11

Paper submitted for presentation at ANS/ENS Conference on Thermal Reactor Safety, October 2-7, 1988, Avignon, France

CONF-881014--11

DE89 000596

RESULTS OF FISSION PRODUCT RELEASE FROM INTERMEDIATE-SCALE MCCI TESTS*

by

B. W. Spencer, D. H. Thompson, J. K. Fink, and W. H. Gunther

Reactor Analysis and Safety Division
Argonne National Laboratory
9700 S. Cass Avenue
Argonne, IL 60439

and

B. R. Sehgal

Electric Power Research Institute
3412 Hillview Avenue
Palo Alto, CA 94303

*Work sponsored by Electric Power Research Institute, Palo Alto, CA, under contract RP 2636-2

RESULTS OF FISSION PRODUCT RELEASE FROM INTERMEDIATE-SCALE MCCI TESTS

B. W. SPENCER, D. H. THOMPSON, J. K. FINK, AND W. H. GUNTHER
(Argonne National Laboratory, USA)
B. R. SEHGAL (Electric Power Research Institute, USA)

ABSTRACT

A program of reactor-material molten core-concrete interaction (MCCI) tests and related analyses are under way at Argonne National Laboratory under sponsorship of the Electric Power Research Institute (EPRI). The particular objective of these tests is to provide data pertaining to the release of nonvolatile fission products such as La, Ba, and Sr, plus other aerosol materials, from the coupled thermal-hydraulic and chemical processes of the MCCI.

The first stages of the program involving small and intermediate-scale tests have been completed. Three small-scale tests (~5 kg corium) and nine intermediate-scale tests (~30 kg corium) were performed between September 1985 and September 1987. Real reactor materials were used in these tests. Sustained internal heat generation at nominally 1 kW per kg of melt was provided by direct electrical heating of the corium mixture. MCCI tests were performed with both fully and partially oxidized corium mixtures that contained a variety of nonradioactive materials such as La_2O_3, BaO, and SrO to represent fission products. Both limestone/common sand and basaltic concrete basemats were used. The system was instrumented for characterization of the chermal hydraulic, chemical, gas release, and aerosol release processes.

Test results have shown first of all that DEH is a successful method for sustaining internal heat generation in molten core materials for long-term MCCI operation. However, the relatively small scale of these tests permitted a stable crust to bridge the apparatus at the top of the interaction zone, restricting the released gas and aerosol to flow through cracks and pores in the crust. MCCI temperature as high as 2400K was measured resulting in concrete ablation which ranged from 0.8 to 3.9 mm/min. The expected H_2O and CO_2 decomposition gasses were measured which accounted for peak superficial velocity of ~4 cm/s. With the metallic zirconium present, CO and H_2 were also measured; there was no evidence of coking. The aerosol consisted mainly of uranium species plus species of concrete decomposition products. The presence of Zr increased measured release fractions of Ba and Sr species by an order of magnitude, and La species by a factor of three.

I. INTRODUCTION

Postulated risk-dominant core melt accident sequences are initiated by postulated faults which result, by definition, in undercooling the core [1]. This in turn leads to core heatup, degradation, eventual melting, and downward relocation of molten core materials (denoted corium). This in-vessel stage of the accident ends when the vessel lower head fails and corium emerges from the vessel. The molten corium consists of UO_2 fuel, zirconium alloy cladding and stainless steel from the vessel internals and their oxides, plus at least the nonvolatile species of fission products. The corium flows from the vessel lower head into the reactor cavity or pedestal region of the containment, initiating the ex-vessel stage of the accident. The corium flow may actually involve a dispersal of the corium to other parts of the containment if the vessel pressure and breach size are such that a vigorous blowdown ensues [2]. Such a sequence involves the possibility that the containment atmosphere may become a significant heat sink for the corium energy. In this paper, however, we address the opposite end of the spectrum, i.e., the corium is retained on the floor of the region beneath the vessel, spreading to fill the available cross section and accumulating in depth dependent on the corium mass and floor area. The possible quenching effect of water or the possible long-term coolability of

the debris if the presence of water can be sustained are not addressed here.

The interaction of the molten corium with the concrete produces several possible effects on the containment and internal systems, notably i) heatup and loss of strength of structural members with possible resultant structural failures and/or containment boundary breach, ii) decomposition of the concrete and possible downward and sideward ablation owing to direct effect of the molten core/concrete interaction (MCCI), iii) release of noncondensable gas to the containment atmosphere which is a long-term pressurization mechanism, iv) release of potentially combustible gasses such as hydrogen to the containment atmosphere, v) release of large aerosol mass, most of which may be inert material, and vi) release in the aerosol of fission product species which have remained with the fuel during the in-vessel melt progression. Investigation of the latter process involving release of nonvolatile fission product species was a particular objective of the EPRI-sponsored MCCI experiment program described here.

OBJECTIVES

The Electric Power Research Institute (EPRI) sponsored at Argonne National Laboratory a series of developmental small-scale tests (5 kg corium) and intermediate-scale gas-sparging and MCCI tests (30 kg corium) to provide a reactor-material data base for integral MCCI processes with emphasis on the fission products released with the aerosol. The specific objectives of the program were as follows:

1. Measure the release of non-volatile (refractory) fission product species (e.g., lanthanum, barium, strontium, etc.) during the molten corium concrete interaction (MCCI).

2. Measure the physical and chemical character of the aerosols generated from the MCCI.

3. Measure the heat transfer in all directions from the molten corium and to the atmosphere; characterize other thermal-hydraulic phenomena during the interaction.

4. Analyze the data obtained in the tests and compare to various analytical predictions.

APPROACH

The key feature of MCCI processes is the sustained internal heat generation in the corium mass. It is the combination of layer depth, internal heat generation, concrete decomposition characteristics, and upward and downward heat transport processes which largely determine the temperature of the melt zone and the concrete ablation. Sparging of the molten corium by concrete decomposition gasses, chemical reactions, and high temperature can all contribute to aerosol and fission product releases. This was mocked up by an experimental technique in which direct electrical heating (DEH) was used for internal heat generation. For MCCI tests, the molten reactor material corium interacted with a concrete basemat. The experiment approach was to employ a configuration emphasizing the one-dimensional (vertical) transport processes rather than two-dimensional, regarded as representative of the interaction in the reactor cavity except for that corium in proximity to walls.

In the long-term erosion stage of MCCI [3], oxidation of metallic species of the corium is essentially complete and internal heat generation is by decay heating only. The oxide melt has been considerably diluted by concrete decomposition products by this time. In the experiments, the oxide layer consisted of UO_2, ZrO_2, Fe_2O_3, Cr_2O_3, NiO, CaO, SiO_2, and nonradioactive mockups of the refractory oxide fission products La_2O_3, BaO, SrO, CeO_2, plus chemical forms of Te as specified for individual tests. The melt layer was in contact with an instrumented concrete slab which was limestone/common sand concrete (Zion composition). Decomposition of the concrete not only introduced CaO and SiO_2 into the oxide layer, but also sparged the melt with H_2O and CO_2 decomposition gasses.

The early aggressive interaction stage of MCCI involves the oxidation of metallic constituents initially present in the corium as the melt is sparged by the concrete decomposition gasses. The oxidation heat source is

a major contributor to the internal heat generation during this interaction stage. Intermediate-scale MCCI tests were conducted to examine the possible enhanced fission product release during this stage owing to reduction of La_2O_3, BaO, SrO, CeO_2, and other normally nonvolatile fission products by H_2 and CO in the sparge gas. (Metal oxidation causes reduction of the H_2O and CO_2 gases to H_2 and CO, respectively.) This was mocked up in the experiment by changing the initial corium composition, such that half of the zirconium was present in metal form.

In addition to the MCCI tests at intermediate scale (20 x 20 cm, 30 kg corium), we have also initiated testing at large scale (50 x 50 cm, 300 kg corium) as part of the internationally sponsored Advanced Containment Experiments (ACE) program [4].

RELATIONSHIP TO OTHER STUDIES

The meaningfulness of such a test program depends upon the development or availability of codes with sufficiently advanced models that comparisons with integral-type tests are warranted. Codes such as CORCON/VANESA [5,6] have been developed for this purpose and are being used in current NRC risk studies [7]. Other related code systems are also under development under IDCOR sponsorship [8] and under EPRI sponsorship [9,10]. The advanced state of these codes, and their application in risk studies, warrants that their predictive capabilities for integral MCCI/fission product release processes be validated by integral-type tests on a timely basis. The EPRI-sponsored experiments at ANL are intended to provide a timely data base for this purpose.

The ANL data base complements the thermal-hydraulic data base from the recent BETA test series which utilized the inductive heating of the iron constituent in an Fe-Al_2O_3 melt in a concrete crucible. The data included sidewards as well as downward concrete erosion [11]. That data had a particularly important influence on the modeling of MCCI interfacial heat transfer processes. The ANL experiments also complement the SNL SURC tests which utilize tungsten susceptor rings heated inductively which are distributed through a reactor material melt to provide internal heating [12].

II. SYSTEM DESCRIPTION

The system for conducting the corium-concrete experiments consisted of a test apparatus, an electric power supply for direct electrical heating of the corium in the test apparatus, a water supply for cooling the test apparatus, a carrier gas system for transporting the off-gases, an aerosol collection and gas sampling system, a ventilation system to filter and exhaust the gases, and a data acquisition system. The test apparatus (Fig. 1) was located within an inerted enclosure in a test cell. A window in the wall of the enclosure permitted the apparatus to be viewed during an experiment via a video camera mounted within the test cell. The use of a water-cooled apparatus, coupled with the low thermal conductivity of the cold corium powder adjacent to the apparatus walls, provided the insulating envelope necessary to contain molten corium for extended test durations.

TEST APPARATUS

The intermediate-scale test apparatus (base dimensions 20 cm by 20 cm) consisted of 10 "U"-shaped brass segments, electrically insulated from each other by zirconia felt, that were stacked together to form the base and sides. Tungsten electrodes, supported in machined electrical insulators, formed the ends of the apparatus. A 25-mm thick blanket of refractory insulation was placed at the top cover.

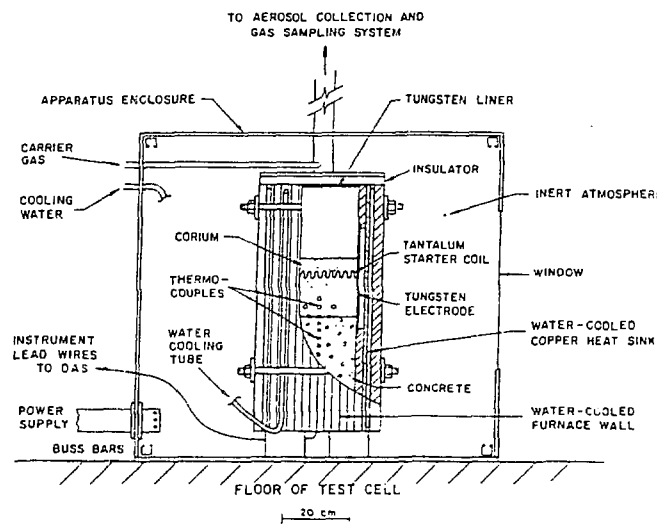

Fig. 1. Apparatus for Intermediate-Scale MCCI Experiments

Power for direct electrical heating of the corium materials was provided by two transformers and associated control gear. A high-voltage, low-current (118 V, ~400 A) transformer provided the low power preheat. Melt operations were sustained using a low-voltage, high-current (48 V, ~2000 A) transformer.

The apparatus was instrumented to monitor and guide experiment operation and to gather data for subsequent evaluation. Parameters monitored included the input power, directional heat losses, corium temperature, carrier gas temperature and flow rate, and temperatures within the concrete basemat. Also input to the data acquisition system were gas temperatures and pressures in the aerosol collection and gas sampling system. These data were logged with a Model 9845B Hewlett-Packard computer operated in conjunction with a 3497A data acquisition/control unit and a 3456A digital voltmeter. The capacity of this system was 80 channels of input data.

A total of seven W5Re/W26Re thermocouples were located at various elevations above or in the region of the basemat in thoria, tungsten, and magnesia thermowells to measure corium temperature. An array of Cr/Al thermocouples in each concrete basemat measured temperatures in the concrete to determine the location of the ablation melt front.

GAS/AEROSOL DIAGNOSTICS SYSTEM

The gas/aerosol diagnostics system used for the latter MCCI tests is shown in Fig. 2. The apparatus cover incorporated a carrier gas injector (diluter) to introduce argon gas into the off-gas line which cooled and diluted the aerosol. The diluter contained a porous stainless steel flow distribution device and a flow straightener to provide a uniform annular gas flow that enveloped the off gas leaving the test cavity. The off-gas piping system contained devices for exposing stainless steel aerosol collection coupons to the main gas stream. Aerosols were collected by diffusion, by gravitational settling, and by impaction. A bank of five lines containing filters and gas sample bottles was operated in sequence to collect aerosol and gas samples at different times during a test to establish the aerosol release rate. The STEP aerosol sampling canister consisted of three chambers with 14 collection stages per chamber [13]. Only one chamber was used for each MCCI test.

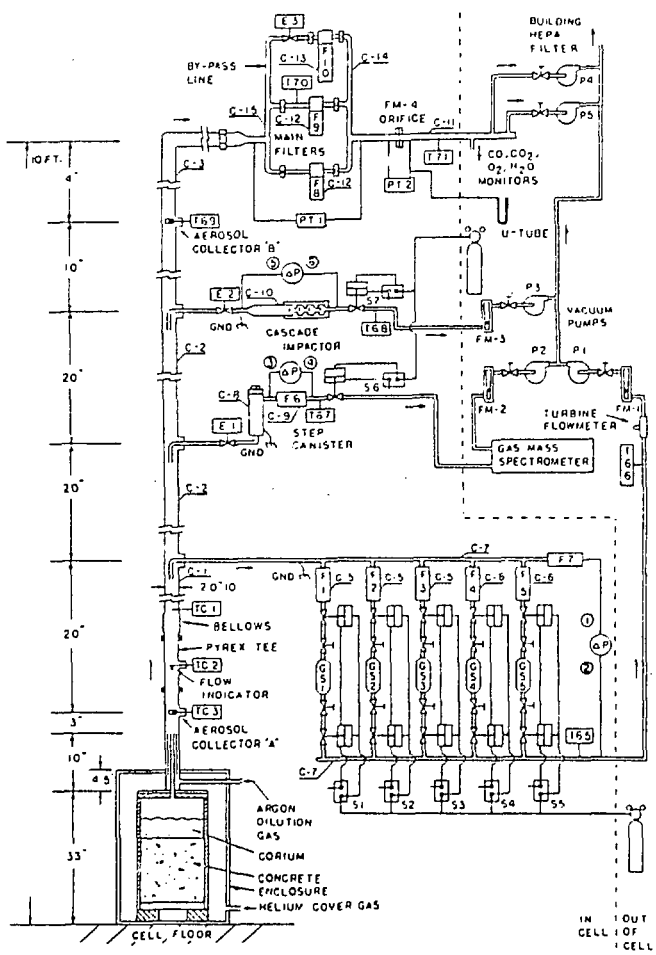

Fig. 2. Gas/Aerosol Diagnostics System

A gas mass spectrometer was used for continuous, on-line analysis of the off-gas composition. Because the dilution gas flowrate was known very accurately, the spectrometer also served as a highly accurate flow meter. A cascade impactor was used for overall determination of the aerosol particle size distribution. An orifice meter was used to monitor the gas flow rate in the main system piping; sample line flowrates were measured with rotameters and turbine flow meter.

A constant 4% isokinetic sample of the main gas flow was drawn through each of the sample lines. The remainder of the gas stream continued through the

main filters (two large cartridge-type glass fiber filters mounted in parallel), past CO, CO_2, and H_2O monitors, and was exhausted through the building scrubber/filtration system.

The argon dilution gas was heated to 100C (373K) before entering the injector. Main system piping, filters, and the sampling subsystems were maintained at 100C (373K) during test operation to preclude moisture condensation. The gas line piping had removable liners in order to determine aerosol losses to the walls and facilitate cleanup.

CORIUM MIXTURE

The corium mixtures for the Intermediate-Scale (I-series) tests are given in Table 1. Through test I-7, the fully oxidized corium composition, representative of materials present in a US PWR, consisted of UO_2 (55%), ZrO_2 (15%), Fe_2O_3 (23%) Cr_2O_3 (6%), and NiO (2%). Trace amounts of La_2O_3, BaO, and SrO were added to simulate the presence of low volatility fission products. Depleted, reactor grade UO_2 in powder or crushed pellet form was used; the other constituents were reagent grade powders. The estimated solidus and liquidus temperatures of this fully oxidized corium were 1350C (1620K) and 2300C (2570K), respectively.

There were variations in the corium composition in the last three tests. The corium for MCCI test I-8 contained CaO and SiO_2 to represent the dilution by concrete decomposition products in reaching the long-term erosion stage of the MCCI. CeO_2 and TeO_2 were added to the simulated fission product inventory. Half the zirconium in the pretest corium inventory for MCCI tests I-9 and I-10 was present as metal. CaO, SiO_2, and CeO_2 were constituents of the I-9 and I-10 corium inventories, which also contained Te metal and Ag-In alloy, respectively. The corium inventories for all the tests were summarized in Table 1.

Table 1. Pretest Corium Inventory in Intermediate-Scale Tests

Constituent	I-1	I-2	I-3*	I-4	I-5	I-6	I-7	I-8	I-9	I-10
	Mass, kg									
UO_2	11.99	11.94	9.92	10.88	11.44	14.67	15.64	10.88	19.04	19.04
ZrO_2	3.19	3.18	2.64	2.89	3.04	3.91	4.17	2.90	2.54	2.54
Zr									1.88	1.88
Cr_2O_3	1.26	1.25	1.04	1.14	1.20	1.53	1.63	1.14		
NiO	0.48	0.48	0.40	0.44	0.46	0.59	0.63	0.44		
Fe_2O_3	5.08	5.06	4.20	4.61	4.85	6.22	6.63	4.61		
CaO								1.26	0.80	0.80
SiO_2								2.02	1.27	1.27
La_2O_3					0.01	0.042	0.045	0.034	0.06	0.06
BaO						0.042	0.045	0.036	0.06	0.06
SrO						0.024	0.026	0.031	0.06	0.06
CeO_2								0.087	0.15	0.15
TeO_2								0.01		
Te									0.02	
Ag										0.39
In										0.07
	22.0	21.91	18.20	19.96	20.99	27.03	28.82	23.44	25.88	26.32

*Failed to reach full power, I-3 corium inventory removed, reconstituted, run as test I-4

CONCRETE BASEMAT

MCCI tests I-5 through I-9 were performed using limestone/common sand concrete with the same aggregates and mix as were used in the construction of the Commonwealth Edison Company's Zion nuclear plant. Ingredients of this concrete include coarse aggregate (45 w/o), sand (32 w/o), Type I Portland cement (14 w/o), fly ash (2.7 w/o), an air entraining admixture, and water (6.1 w/o). Only the gravel that passed a 19.1-mm (3/4-in.) sieve, which ranged from 84 to 100% of the total from the Zion quarry, was used.

The chemical composition of the limestone/common sand and basaltic concretes used in these tests are listed in Table 2. Concrete for the test basemats was mixed in a cement mixer using the ASTM C 192 mixing procedure. The concrete was placed into plastic-lined forms and was vibrated and tamped during each 4-cm concrete addition until the full 30.5-cm depth was

Table 2. Chemical Composition of Limestone/Common Sand and Basaltic Concrete Used in Intermediate-Scale Tests

Constituent	Chemical Composition, w/o Limestone/Common Sand	Basalt
SiO_2	38.3±1.3	42.1±1.8
TiO_2	0.04±0.01	0.02±0.01
MgO	8.2±1.7	6.3±1.0
CaO	24.1±1.5	15.0±1.0
Na_2O	0.05±0.08	3.2±0.9
K_2O	0.09±0.09	0.08±0.08
FeO	0.0	11.2±1.6
Fe_2O_3	0.8±0.1	0.4±0.1
Al_2O_3	1.7±0.3	15.?±1.9
CO_2	20.3±2.3	trace
H_2O (evap)	4.2±1.0	4.1±1.0
H_2O (bound)	2.0±1.0	2.1±1.0
SO_3	0.24±0.01	0.2±0.01

reached. One multi-thermocouple array was located in the center of each form. This array and the other thermocouples in their thermowells were carefully supported during placement of the concrete. Each form was sealed in plastic and the concrete cured for a month. On removal from the form, the concrete was aged a minimum of 45 days before use.

MCCI Test I-10 was performed with a basaltic concrete basemat. Basaltic aggregate and washed sand were obtained from Dresser Trap Rock, Dresser, Wisconsin.

TEST OPERATION

A test was begun by slowly increasing power input to the test apparatus from the preheat power supply. As the corium powder was heated by the tantalum coils, the electrical conductivity of the powder increased, and at about 1000C operation was shifted to the high power supply. The corium powders typically sintered and subsequently melted during this process, starting first at the heater coils. The melt region grew as operation continued, consolidating into a pool leaving sintered crust and powders on the cooled walls, and leaving a sintered crust spanning the top in these small-scale tests. Eventually the melt region extended over the entire cross section of the apparatus except for the crusts on the cooled walls and extended completely to the bottom of the powders. The onset of melt/concrete interaction was quite abrupt and readily detected both from thermocouple data as well as off-gas composition.

During test operations, the heat losses through each face of the apparatus were determined continually. The gross power was automatically increased to compensate for heat losses to sustain nominally 1 kW/kg net heat input into the corium melt. Adjustments were made principally in pump suction to hold the main- and sample-line gas-flow rates constant for isokinetic sampling purposes. Pressure drops across individual gas-sample-line filters were monitored to aid in control of the aerosol collection intervals.

III. EXPERIMENT RESULTS

Three small-scale and nine intermediate-scale tests were completed during the period from September 1985 through September 1987. These tests are characterized in Table 3.

Results of I-series MCCI tests through the I-7 tests have been previously published in Refs. 3 and 14. Comprehensive results for all tests are presented in Ref. 15. Results for previously unreported test I-8 are described here. Findings from the overall investigation, including the recent I-9 and I-10 tests are summarized in the following section.

Table 3. Matrix of Intermediate-Scale Tests

	I-1	I-2	I-3/I-4	I-5	I-6	I-7	I-8	I-9	I-10
Test Type									
nonsparge	X	X							
gas sparge			X						
MCCI				X	X	X	X	X	X
Corium									
fully oxidized	X	X	X	X	X	X			
fully oxidized w/CaO, SiO_2							X		
contained Zr metal								X	X
Concrete Basemat									
limestone/common sand				X	X	X	X	X	
basalt									X
Internal Heat Generation				(1)	(2)	(3)	(3)	(4)	(3)

(1) Net power increased in steps from 0.8 to 20 kW/kg
(2) Net power decreased from 2.7 to 0.4 kW/kg
(3) Constant net power of ~1 kW/kg
(4) Constant net power of ~0.5 kW/kg

MCCI test I-8 investigated the interaction of fully oxidized core melt material with limestone/common sand concrete. The pretest corium inventory contained 14 w/o CaO and SiO_2 to represent the corium dilution by concrete decomposition products in reaching the long-term erosion stage of the MCCI. The pretest corium inventory amounted to 23 kg. The weight of SiO_2 in the corium was 1.6 times that of the CaO based on the composition of the limestone/common sand concrete being used. CeO_2 and TeO_2 were added as fission product species for this test in addition to the Ba, La, and Sr oxides used in all tests. For detection purposes, the concentration of all fission product mockups was twice that in a LWR.

The net power into the corium (total power input less the heat loss through the four water-cooled sides of the apparatus) was maintained at 10 kW after full power operation was achieved. The interaction of molten corium with the concrete began at 100 min into the test. This was indicated by an abrupt change in gas composition, an increase in pressure drop across the main filters, an 110C increase in crust temperature, and a jump in the gas temperature above the corium from 42C to 66C. During the first 15 min of basemat erosion, the temperature of the off gas leaving the test apparatus further increased to 90C.

The time history of the gas composition is shown in Fig. 3. Upon start of MCCI at 100 min, the CO_2 concentration increased to about 18 v/o in the gas stream. This jump in concrete decomposition gas displaced inflow of helium from the inerted ambient environment such that the total volumetric flow remained constant in the gas system for isokinetic sampling purposes.

Temperatures in the basemat increased as the melt front advanced. The signal from the W5Re/W26Re thermocouple that protruded 17.5 mm into the corium volume from the basemat (T45) plateaued at 1544C (1817K) for three minutes (117.2 min to 120.2 min), as shown in Fig. 4. Higher temperatures were reached by thermocouples in the concrete basemat, 1698C (1971K) at -9 mm (T40) (116.5 min.) and 1628C (1901K) at -24 mm (T46) (137.7 min).

Posttest disassembly revealed that appreciable molten material had been lofted to above the upper surface of the corium overcrust during test I-8. There were a number of eruptions penetrating the crust, two of which had grown high enough to reach the under side of the top cover. There was no collapse of the overcrust in this test as there was in tests I-5 and I-10.

The melt layer thickness measured about 60 mm. A high gas porosity was found in the upper half of the melt layer. The density of porous melt sam-

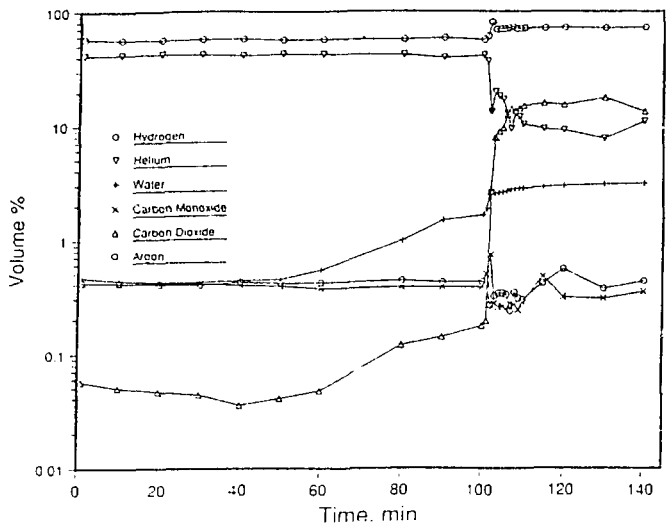

Fig. 3. I-8 Gas Stream Composition

ples "foil wrapped" and "unwrapped" measured 1.9 g/cm^3 and 3.6 g/cm^3, respectively. There was little porosity evident in the melt material immediately above the concrete. The density of this material measured 4.3 g/cm^3.

After the corium layer had been removed, the remaining concrete was weighed. Weight of the concrete decreased from 33.78 kg to 27.37 kg. The corium weight increased from a pretest value of 23.44 kg to 27.85 kg. Hence there was a net change in weight of the interacting materials which amounted to a loss of 2.0 kg.

An evaluation was made of the origin of the measured weight loss. For limestone/common sand concrete, 73.1 w/o of the decomposed concrete would enter the melt and 26.9 w/o would be released as a gas. In addition, moisture released by dehydration of concrete ahead of the melt front would also contribute to weight loss of the basemat. In test I-8, the 100C (373K) isotherm reached a maximum depth of 152.4 mm (6 in.) in the basemat 1.5 hours after power operation ended. The water content of the concrete was 6.22 w/o (4.22 w/o free, 2.0 w/o bound). Dehydration of unablated concrete was considered to free only the unbound water.

The following mass balance results were obtained:

Average ablation depth	53.8 mm (2.12 in.)
Concrete constituents into melt	4.35 kg
CO_2, SO_3 evolution from concrete ablated	1.22 kg
Free and bound H_2O from concrete ablated	0.37 kg
Free H_2O from dehydrated concrete	0.46 kg

The calculated 53.8-mm (2.12-in.) ablation depth, 4.35-kg solid material uptake from concrete into the core melt debris, and 2.05-kg gaseous release from the interaction are in excellent agreement with the measured results.

An estimate was made of the posttest corium composition based on the pretest composition together with the addition of 4.35 kg of concrete decomposition products. This composition, shown in the last column of Table 4, assumed all materials were uniformly distributed.

Samples of core melt debris taken at several elevations in the melt and from the underside of the overcrust were chemically analyzed. The composition of the solidified corium from these locations is also shown in Table 4. Some constituents of the melt appear to be uniformly distributed throughout whereas others show clear evidence of segregation. The UO_2 concentration was

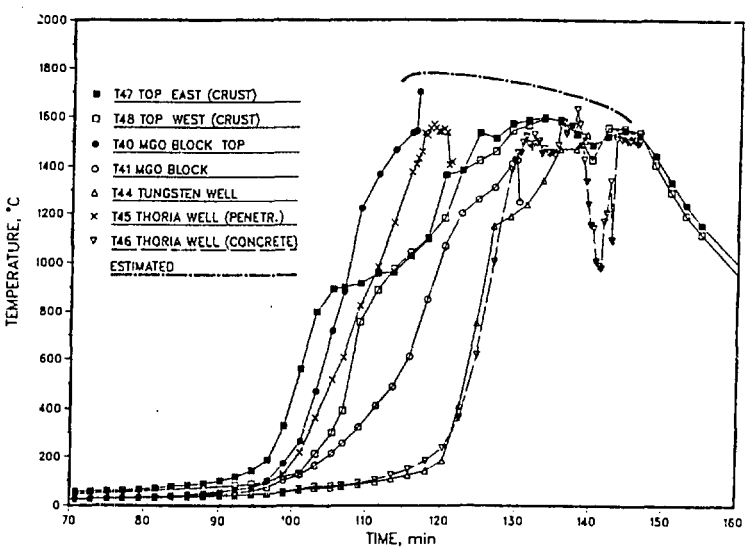

Fig. 4. I-8 MCCI Melt Layer Temperature Measurements

Table 4. Constituents in MCCI Test I-8 Corium and the Melt Material

Constituent[a]	Composition, w/o				
	Pretest Corium Powder	Underside of Overcrust	Melt Layer Top	Melt Layer Bottom	Posttest Corium
UO_2	46.41	35.43	34.48	45.91	39.26
ZrO_2	12.36	8.50	6.97	7.28	10.47
Cr_2O_3	4.85	5.28	2.72	2.38	4.11
NiO	1.87	1.65	1.29	1.23	1.59
Fe_2O_3	19.68	16.33	15.08	12.24	16.82
CaO	5.38	10.09	12.56	9.54	9.74
SiO_2	8.61	14.96	18.96	14.01	15.52
BaO	0.15	0.13	0.12	0.09	0.13
La_2O_3	0.15	0.08	0.09	0.06	0.12
SrO	0.13	0.10	0.10	0.09	0.11
TeO_2	0.045	-	-	-	-
CeO_2	0.37	-	-	-	-
Al_2O_3		4.13	3.91	4.10	0.36
MgO		3.24	3.60	2.99	1.77
MnO		0.07	0.07	0.06	

[a]an oxide form was assumed for all constituents

greater at the bottom of the melt than at the top. Conversely, the concentration of some low-densityconstituents, such as CaO and SiO_2, were higher at the top of the melt than at the bottom. ZrO_2 is lower than expected. The presence of Al_2O_3 and MgO is higher than expected, probably due to the use of alumina and magnesia thermowells.

DECOMPOSITION GAS/AEROSOL CHARACTERIZATION

Gas stream aerosol concentrations determined from filter and substrate weight changes during test I-8 are shown in Table 5. A total of 3.8 kg of

Table 5. Aerosol Collection and Concentration in MCCI Test I-8

	Mass Collected, mg	Collection Interval, min	Average Aerosol Concentration, g/m^3 (STP)	Off Gas Fraction	Average Aerosol Concentration, g/m^3 off gas (STP)
Main filters	2901	150	0.36		
Filter/ gas bottle array					
Filter 1	14.2	100	0.06	0.00	
Filter 2	27.6	10	1.18	0.10	12.1
Filter 3	27.1	10	1.16	0.15	7.8
Filter 4	30.1	10	1.29	0.17	7.8
Filter 5	25.5	10	1.09	0.16	7.0
Total	124.5	140	0.38		
Filter after STEP canister	104.4	150	0.31		
Cascade impactor (eight substrates plus filter)	101.4	150	0.31		
Liners and Pyrex tee	582.7	150			

aerosol material was collected of which about 90% was released during the 40-min ablation period. The aerosol concentration remained relatively constant at ~1.2 g/m^3 (STP) of total flow in the gas system during the actual ablation period (filters 2-5). The fraction of the total gas flow which is decomposition gas and the aerosol concentration transported by the decomposition gas are also shown in Table 5. That aerosol concentration was 12 g/m^3 (STP) of off gas during the first 10-min period and about 7 to 8 g/m^3 (STP) of off gas during the subsequent 30 min. The superficial gas velocity determined from the off-gas flow rate and the estimated temperature of the corium melt was about 33 mm/s.

Aerosol particles were collected using a Sierra cascade impactor to determine mass distribution according to particle size. Eight stages were used during test I-8. In addition, there was a final filter within the impactor body to collect the submicron particles that passed the last stage. Glass fiber substrates were used as collection surfaces. In test I-8, most of the mass collected in the Sierra cascade impactor was found on the final filter.

The percent mass less than a given aerodynamic mass median diameter (AMMD) for test I-8 (and I-9) is shown in Fig. 5. Neither set of test data shows a bimodal distribution. The AMMDs were determined by the intersection of the curves in Fig. 5 with the 50th percentile. The slope of the curves gives the geometric standard deviation (GSD). For test I-8, the AMMD was 0.2 μm and the GSD was 6.1.

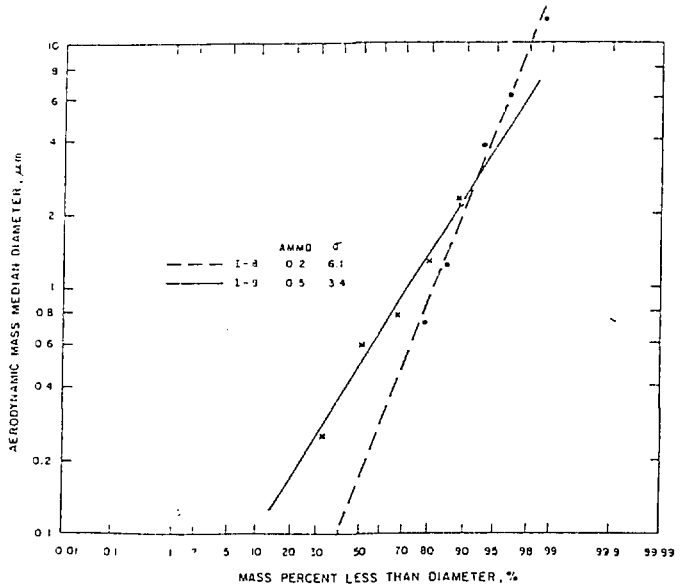

Fig. 5. Aerosol Size Distribution

AEROSOL CHEMICAL ANALYSIS

Aerosol samples were chemically analyzed using inductively coupled plasma-atomic emission spectrometry (ICP-AES), fluorescence, and atomic absorption spectrophotometry (AAS). Samples were analyzed from the impactor substrates so information could be obtained on composition as a function of particle size.

Because fiberglass substrates were used in the impactor, the silica content of the aerosol deposits could not be quantitatively determined by chemical analysis. Tabulated values of silica were determined by difference. The overall composition of the aerosols was determined from the composition of particles in each size range by a mass average.

Three impactor samples from MCCI test I-8 were analyzed. Samples collected on substrates from stages 4 and 7 in the cascade impactor and the final filter in the cascade impactor had particles AMMDs in the size ranges 5-8 μm, 0.9-1.7 μm, and less than 0.6 μm, respectively.

Results of analysis of the large particles were consistent with SEM/EDX examinations of large particles on main line coupons and on wires and settling plates from the STEP canister. Significant amounts of both uranium and zirconium were present in large particles (such as spheres observed by SEM/EDX). Tellurium was detected in all size ranges but the largest mass of tellurium was in the submicron size range. A small amount of cerium was detected (12.9 μg); it had an AMMD less than 0.6 μm. Slightly more barium, strontium, and lanthanum were detected. These elements were found mainly in particles smaller than 0.6 μm with only a small percent present in the 0.9-1.7 μm AMMD size range. Only a small fraction of the fission product inventory was released as aerosols.

From the chemical composition of aerosols for three size ranges, the overall composition of the collected aerosols was determined by a weighted average of the composition in each size range. The error in estimating the

entire composition from the composition of three size ranges and the mass fraction in each size range was determined to range from 4 to 69% with an average error of 24%. The largest error (69%) was for lanthanum oxide, which had the smallest release. The overall aerosol composition determined for test I-8 is given in Table 6. Using this overall composition and the total aerosol mass released (as determined from masses collected on filters, liners, and impactors), the release fraction of each specie was also determined and is also given in Table 6. Note that the species were listed here according to their chemical form in the pretest corium inventory. The actual chemical form in the aerosol may be different.

Table 6. Summary of Aerosol Release Data for Test I-8

	Percent of Inventory Released	Percent of Overall Aerosol Composition
UO_2	2.3×10^{-3}	6.5
BaO	3.1×10^{-3}	2.8×10^{-2}
SrO	4.5×10^{-3}	3.7×10^{-2}
La_2O_3	2.4×10^{-3}	2.1×10^{-2}
CeO_2	9.2×10^{-4}	2.0×10^{-2}
TeO_2	27.1	71.1
SiO_2	1.6×10^{-4}	1.9
CaO	1.2×10^{-2}	9.0
MgO	1.8×10^{-2}	2.4
Al_2O_3	3.7×10^{-1}	8.1
Fe_2O_3	4.1×10^{-4}	0.5
Total percentage		99.6

IV. SUMMARY OF FINDINGS

The following specific findings regarding the physical processes of the MCCI and the aerosol and fission product releases are based on the results of MCCI tests I-5 through I-10.

1. Direct electrical heating was a successful means of initiating a core debris melt involving real reactor materials and providing sustained internal heat generation in the melt through extended core concrete interaction, including corium mixtures in which metal was present as a constituent.

2. There was a crust formation that bridged the top of the test cavity in the intermediate-scale apparatus that was not prototypic of MCCI conditions. This crust had the effect of a heat shield and also restricted gas flow and aerosol release. In two of the six MCCI tests, the crust collapsed into the melt under its own weight.

3. A vigorous mechanical agitation of the melt occurred during ablation for all concrete and corium compositions tested. The peak superficial gas velocity was ~4 cm/s.

4. Ablation rates between 0.8 and 3.9 mm/min were measured in the intermediate-scale MCCI tests. The rates were influenced by the power level, the corium melt temperature, and the uptake of concrete decomposition products into the melt. Exothermic oxidation of zirconium metal in the corium elevated the melt temperature above that reached by sustained internal heat generation; the peak temperature in MCCI test I-10, determined from thermocouple data, was 2150C (2420K).

5. The presence of zirconium in the corium melt and the type of concrete used in the tests both had an effect on the composition of the off gas. For a fully oxidized melt and limestone/common sand concrete, the off gas consisted almost entirely of CO_2 and H_2O, whereas for a melt initially containing zirconium metal, H_2 and CO constituted about 50% of the off-gas volume. Lack of carbonates in basaltic concrete yielded an off gas of H_2 and H_2O.

6. The type of concrete determined the volume of off gas. In MCCI tests I-8 and I-9 with limestone/common sand concrete, the off-gas production was ~0.07 m^3(STP)/kg of basemat weight loss. In MCCI test I-10 with basaltic concrete, the off-gas production was 0.027 m^3(STP)/kg of basemat weight loss, only 40% of that from limestone/common sand concrete.

7. Basaltic concrete yielded a larger aerosol mass than limestone/common sand concrete. Aerosol transport from ablation of limestone/common sand concrete was 0.45 g/kg of basemat weight loss. For basaltic concrete, the aerosol transport was ≥0.52 g/kg of basemat weight loss.

8. No evidence of coking was found in any of the MCCI tests according to observations of the CO_2 and CO composition in the off gas.

9. Neglecting aerosols created by volatile fission products (Te, TeO_2) and volatile control-rod materials (Ag, In), the major constituents of the aerosols released, on a mass basis, were calcium, aluminum, and uranium in MCCI test I-8, in which fully oxidized corium eroded limestone/common sand concrete; uranium, silicon, and calcium in MCCI test I-9, which had zirconium metal in the corium eroding limestone/common sand concrete; and silicon in MCCI test I-10, which had zirconium metal in the corium eroding basaltic concrete.

10. Neglecting the aerosols from the volatile fission products and control-rod materials, the fission products comprised approximately 1 w/o of the aerosol inventory.

11. With the presence of zirconium metal in the corium inventory, the fraction of BaO and SrO released was increased by an order of magnitude; the fraction of La_2O_3 released was increased by about a factor of 3.

ACKNOWLEDGMENTS

This work was sponsored by Electric Power Research Institute under Contract No. RP 2636-02. This work benefited from helpful interactions with D. Bradley (SNL), J. Brockman (SNL), B. Burson (USNRC), M. Corradini (Univ of Wisc), G. Greene (BNL), M. Kazimi (MIT), and D. Powers (SNL). The authors are indebted to D. Armstrong, D. Kilsdonk, R. Aeschlimann, and R. Wesel for their important contributions to this program. The manuscript was prepared for publication by V. Eustace.

REFERENCES

1. B. R. Sehgal and J. J. Carey, "Degraded Core Accidents - An Overview," Proc Intl Mtg LWR Severe Accident Evaluation, Cambridge, MA, Aug 28-Sept 1, 1983. American Nuclear Society (1983).

2. B. W. Spencer, J. J. Sienicki, M. Merilo, and B. R. Sehgal, "Results of EPRI/ANL DCH Investigations and Model Development," Proc Intl Conf on Thermal Reactor Safety, Avignon, France, Oct 2-7, 1988.

3. B. W. Spencer, W. H. Gunther, D. R. Armstrong, D. R. Armstrong, D. H. Thompson, M. G. Chasanov, and B. R. Sehgal, "EPRI/ANL Investigations of MCCI Phenomena and Aerosol Release," OECD CSNI Specialist Meeting on Core Debris/Concrete Interactions, Palo Alto, CA, Sept 3-5, 1986, EPRI NP-5054-SR, pp. 3-25, Feb 1987.

4. F. J. Rahn, R. C. Vogel, and A. Rubio, "EPRI Severe Accident Research Programs," Proc Intl Conf on Thermal Reactor Safety, Avignon, France, Oct 2-7, 1988.

5. R. K. Cole, D. P. Kelly, and M. A. Ellis, "CORCON-Mod2: A Computer Program for Analysis of Molten-Core/Concrete Interactions," NUREG/CR-3920, SAND84-1246 (1984).

6. D. A. Powers, J. E. Brockman, A W. Shiver, "VANESA: A Mechanistic Model of Radionuclide Release and Aerosol Generation During Core Debris Interactions with Concrete," NUREG/CR-4308, SAND85-1370 (1985).

7. Reactor Risk Reference Document (Draft), NUREG-1150, USNRC, Washington, DC (1987).

8. M. G. Plys, M. A. Kenton, and R. E. Henry, "Ex-Vessel Fission Product Release Modeling Within Integrated Accident Analysis," OECD CSNI Specialist Meeting on Core Debris/Concrete Interactions, Palo Alto, CA, Sept 3-5, 1986.

9. M. Lee and M. S. Kazimi, "Modeling of Molten Corium-Concrete Interaction," EPRI NP-5403 (1987).

10. J. K. Norkus and M. L. Corradini, "Modeling of Molten-Core/Concrete Interactions: Fission Product Release," Proc Intl Conf on Thermal Reactor Safety, Avignon, France, Oct 2-7, 1988.

11. H. Alsmeyer et al., "BETA Experimental Results on Melt/Concrete Interaction," OECD CSNI Specialist Meeting on Core Debris/Concrete Interactions, Palo Alto, CA, Sept 3-5, 1986.

12. E. R. Copus and R. Blose, "Sustained Uranium-Concrete Interactions: The SURC Experiments," OECD CSNI Specialist Meeting on Core Debris/Concrete Interactions, Palo Alto, CA, Sept 3-5, 1986.

13. B. J. Schlenger et al., "The Source Term Experiments Project Deposition Sample Characterization," EPRI NP-4967 (1986).

14. B. W. Spencer, D. H. Thompson, D. R. Armstrong, J. K. Fink, W. H. Gunther, D. J. Kilsdonk, and B. R. Sehgal, "Investigation of Molten Corium-Concrete Interaction Phenomena and Aerosol Release," 24th ASME/AIChE National Heat Transfer Conference, Pittsburgh, PA, August 9-12, 1987.

15. D. H. Thompson, J. K. Fink, and B. W. Spencer, EPRI NP-series report, in press.